Low-Power BTO on SiN MZI Weights for Neuromorphic Photonics

T. Chrysostomidis(1,4), D. Chatzitheocharis (1,4), F. Eltes(2), C. Convertino(2), T. Buriakova(3), M. Zervas(3) and K. Vyrsokinos(1,4)

(1) School of Physics, Aristotle University of Thessaloniki, 54124, Thessaloniki, Greece, tchrysos@auth.gr
(2) Lumiphase, AG, Laubisrütistrasse 44, 8712 Stäfa, Switzerland
(3) Ligentec SA, CH1024, Ecublens, Switzerland
(4) Center for Interdisciplinary Research & Innovation, Aristotle University of Thessaloniki, 57001, Thessaloniki, Greece, AUTH

Abstract *We present a BTO on Si_3N_4 MZI as an optical weight for Neuromorphic Photonics featuring ultra-low power consumption of 121 nW for π phase shift, a $V_\pi L$ product of 2.94 Vmm, extinction ratio higher than 27 dB, and less than 20 ns rise/fall time. ©2023 The Author(s)*

Introduction

Neuromorphic photonics is an emerging field that aims to develop artificial intelligence (AI) systems featuring several advantages over electronic counterparts, including higher speed and bandwidth [1], lower power consumption [2], and higher parallelism [3]. One of the key components in neuromorphic photonics is the weighting element that controls the strength of the connections between neurons. These elements must possess high precision, low power consumption, and fast response times to enable efficient and accurate neural network operation at ultra-high speed. Implementing weights in Si photonics is rather tricky because such devices usually lead to high-power consumption or low extinction ratios. Among the various material platforms Si_3N_4 has emerged as the most promising one due to its unique combination of low optical losses and low cost. The weights in the majority of the demonstrators though are implemented by thermo-optic Phase Shifters (PSs) with a power consumption usually higher than 60 mW at 1550 nm [4]. Phase change materials have managed to negate power consumption introducing a thermo-optic coefficient as low as $0.1\times10^{-3}K^{-1}$ in the crystalline phase but the extinction ratio has been as low as 18 dB [5]. Going now to other low power technologies, stress-optic phase actuators have reduced power consumption to 1 μW, but the half-wave voltage-length ($V_\pi L$) is as high as 16 Vcm [6]. Graphene phase shifters also recently exhibited a $V_\pi L$ of 6.9 Vmm with 3.2 dB insertion losses, while SiN loaded on LNOI phase shifters led to insertion losses of 0.5 dB but low extinction ratio of 10.5 dB [7]. Finally, SiN loaded on BTO thin films led to optical weights with a 106 nW/FSR power consumption in ring resonators. Nevertheless, due to the resonator design, the operation of such a weight is wavelength dependent and the extinction ratio was only 6 dB [9].

In this paper, we report on the experimental investigation of the performance of Barium Titanate Oxide (BTO) integrated on top of Silicon Nitride (Si_3N_4) MZIs as weight elements for neuromorphic computing. Our results demonstrate that BTO-Si_3N_4 MZIs can achieve ultra-low power consumption of 121 nW for a π phase shift, a high extinction ratio of over 27 dB, a $V_\pi L$ product as low as 2.94 Vmm, and rise/fall times below 20 ns, making them highly suitable for weight elements in photonic neural networks. We also analyze the trade-off between losses and the $V_\pi L$ product of the MZIs resulting from the interface between the two materials.

SiN-BTO Interface description

Fig. 1(a) illustrates a 3D schematic of the Si_3N_4-BTO interface, that consists of two coupling steps: (a) an end-fire step from Si_3N_4 to the

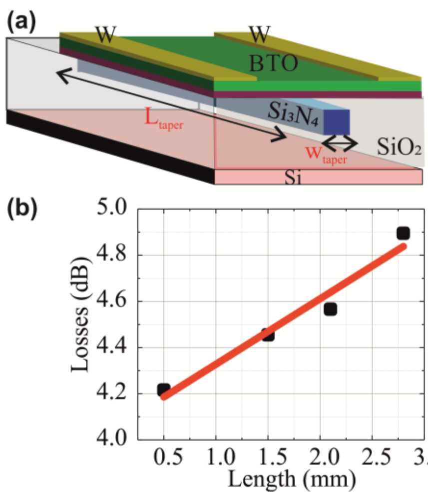

Fig. 1: a) Schematic layout of the BTO-Si_3N_4 PS, (b) Losses at maximum transmission point vs phase shifter length of the MZI structures and linear fitting.

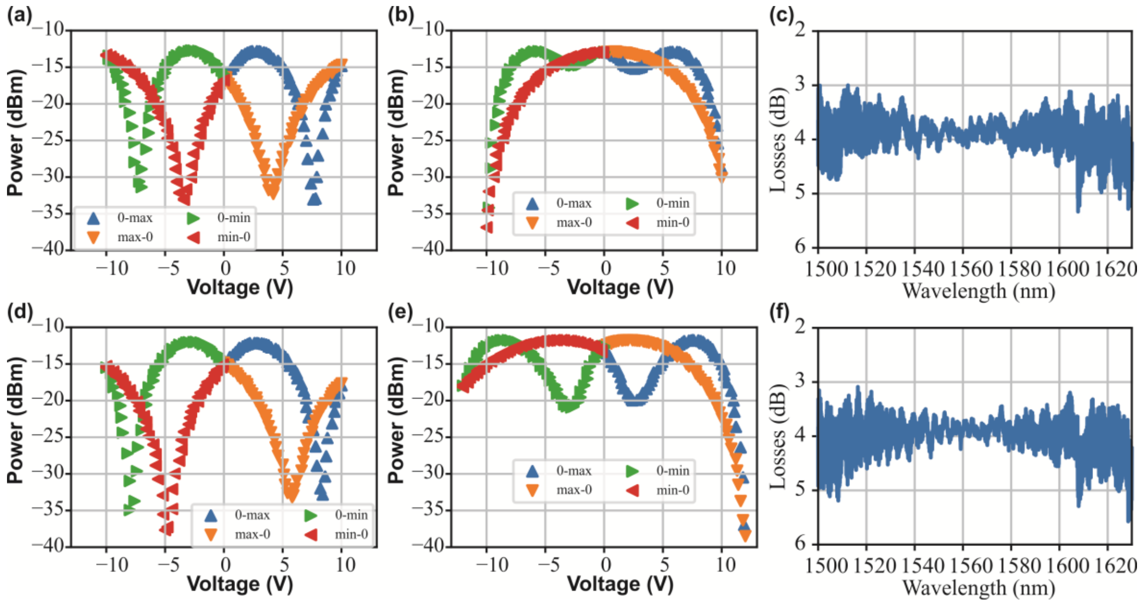

Fig. 2: (a) Down and (b) Up PS transfer function for circular voltage sweep between -10V and +10V for MZI 1 (w_{SiN} tip = 500 nm), (c) wavelength transfer function at maximum transmission point (2.8V at Down PS), (d) Down and (e) Up PS transfer function for circular voltage sweep between -10V and +10V for MZI 2 (w_{SiN} tip = 700 nm), (g) wavelength transfer function at maximum transmission point (2.8V at Down PS)

Si_3N_4-BTO waveguide that excites the targeted hybrid mode residing in both the Si_3N_4 and BTO layers, and (b) an adiabatic taper that excites a mode with a substantially higher power percentage in the BTO layer, suitable for energy efficient phase-shifters (PSs). The variation of the width of the Si_3N_4 taper leads to a trade-off between propagation losses to the Si_3N_4-BTO PS and power efficiency. For a 500 nm Si_3N_4 tip width and 70 μm adiabatic coupling length, the 3D-FDTD simulations revealed a coupling loss of 1.62 dB per interface. Fig. 1(b) shows the cutback measurements from four such MZIs with PS lengths of 0.5 mm, 1.5 mm, 2.1 mm, and 2.8 mm. The linear fitting of the losses reveals a slope of 0.28 dB/mm and an intercept of 4.04 dB. This value includes the two interfaces and the two MMIs with nominal losses of 0.22 dB per device. Therefore, the experimental losses per interface can be calculated as 1.8 dB, very close to the theoretical calculated value.

The role of the Si_3N_4 taper width in the performance of the MZI weight is investigated by comparing the performance of two identical MZIs featuring the same 0.7 mm long PS. Fig. 2(a)-(c) presents the performance of MZI_1 with 500 nm Si_3N_4 taper width, while Fig. 2(d)-(e) the corresponding measurements from MZI_2 with 700 nm taper width. From Fig. 2(a),(b) it is clear that the two PSs of the MZI do not have the same performance and the analysis will focus on the Down PS exhibiting superior performance. The transfer function was extracted by sweeping the voltage from 0 V to a maximum of 10 V, then reducing it to -10 V through the 0 V point and reversing it back to 0 V. Figure 2(a) displays the hysteresis loop characteristic of the ferroelectric properties of BTO. Going from 0 V to +10 V and -10V, the V_π is equal to 4.78 V and 4.2 V, respectively. Going from maximum values ± 10V to 0 V, the V_π cannot be extracted unless transferring between positive and negative voltages. In this case, the V_π is 6.15 V for increasing values and 7.11 V for decreasing ones. With a 0.7 mm PS length, the best result achieved is 2.94 Vmm. The extinction ratio from +7V to +2.8V is over 21 dB, enabling the weighting of input signals at a wide power range. The Up PS, on the other hand, shows no significant power attenuation until the voltage reaches the limit of ±10 V. There is some power deviation when going from 0 V to ±3 V, but the extinction ratio is less than 3 dB, which is not suitable for neuromorphic photonics. Figure 2(c) displays the wavelength transfer function by sweeping the laser source from 1500 nm to 1630 nm, with 2.8 V applied to the Down PS. The transfer function is normalized by subtracting the losses of the reference waveguide. The loss at 1550 nm is 4.146 dB, with an expected value of 4.235 dB according to Figure 1(b). The absolute minimum loss is 3 dB at 1512.35 nm. The ripples in the transfer function originate from the reflections at the two facets of the chip recorded at the reference waveguide and transferred to Fig. 2(c).

Fig. 2(d), (e) present the optical power transfer function for MZI_2 now by varying the voltage at Down and Up PS, respectively. The voltage sweep follows the same pattern as for MZI_1 and reveals again the hysteresis loop for both positive and negative values. Going from

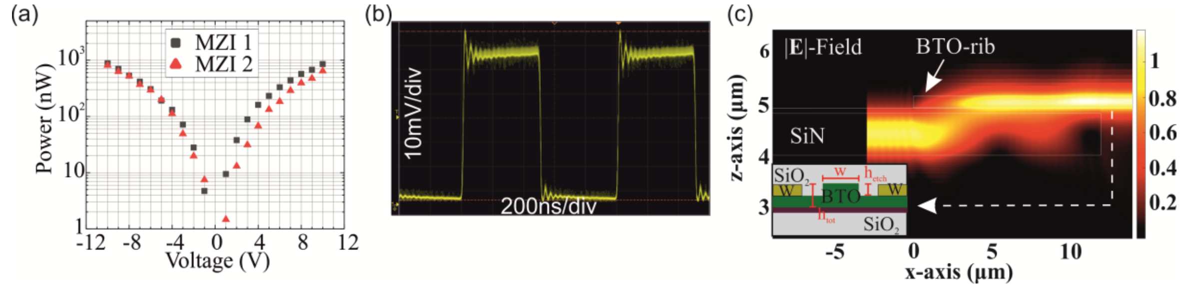

Fig. 3: a) Electrical Power consumption vs Applied Voltage for MZI 1 and MZI 2, (b) Optical time response of MZI1 when driven with 1MHz square pulse, (c) electric field distribution **|E|** taken with 3D-FDTD simulations for optimized interface with rib BTO waveguide. The inset shows the cross section of the BTO.

0 V to +10 V the V_π is 5.6V, while from 0 V to -10 V, the V_π is 5.6 V. On the other hand, when the voltage is decreased from max ±10 V to 0 V, the V_π can only be determined by moving from positive to negative voltages and vice versa, where it equals 7.8 V and 8.6 V, respectively. Overall, the best $V_\pi L$ product is measured now to 3.92 Vmm that is 33% higher from MZI_1. This comes from the Si_3N_4 taper that excites a mode more confined to the Si_3N_4 layer and overlapping less with the W electrodes, propagating in the BTO-Si_3N_4 PS. The Up PS, on the other hand, shows no significant power attenuation until the voltage reaches the limit of ±10 V. However, there is some power deviation when going from 0 V to ±2.8 V, but the extinction ratio is less than 8.2 dB. Fig. 2(f) shows the wavelength transfer function by sweeping the laser source from 1500 nm to 1630 nm, when 2.8 V is applied to Down PS. The transfer function is normalized, which means that the losses of the reference waveguide have also been subtracted. The loss at 1550nm is 3.804 dB, which is 0.3dB higher than that of MZI1. The minimum loss in the entire recorded spectrum is 3 dB at 1516.55nm. The ripples are due to the same reason as in Fig. 3(c).

Figure 3(a) shows the results of the electrical power drawn by one phase shifter (PS) for MZI_1 and MZI_2 versus the applied voltage. The power consumption is almost identical for positive or negative voltages, ranging from a few nW between -3 V and 3 V to a maximum of 1 μW for ±10 V. The comparison of the two MZIs reveals almost identical behaviour, indicating a stable electrical performance of the BTO material. The V_π value obtained from this graph is 123 nW, which sets a record number for non-resonant weighting devices on the Si_3N_4 platform.

Figure 3(b) shows the optical response of MZI1 when driven with 1 MHz pulses at 6 V_{pp} voltage and 4.5 V biasing. The signal is applied through DC wires, the bandwidth of the pulse pattern generator (PPG) is 20 MHz, and the signal is recorded with a 70 MHz oscilloscope. The horizontal time scale is 200 ns/div, which reveals a rise/fall time of less than 20 ns for the time response, implying an operation speed of over 50 MHz.

The overall losses of the proposed MZI weighting elements can be significantly reduced by improving the processing of the Si_3N_4/BTO interface. Etching the BTO layer to form rib waveguides can support optical modes confined solely in the BTO layer, thereby decreasing the $V_\pi L$ metric. For optimal performance, the BTO rib should have a width of 1 μm and an etching depth of 120 nm. The interface should follow a Si_3N_4 waveguide width that decreases from 800 nm to 200 nm, and the BTO rib width should increase from 200 nm to 1 μm in 12 μm. Figure 3(c) shows the simulated sideview of the electric field distribution **|E|**, obtained with 3D-FDTD simulations, demonstrating an overall loss of less than 0.18 dB per interface. Assuming a DAC that is capable of generating ±6 V analog signals and taking into account the measured 2.94 $V_\pi L$ product, the overall losses of each MZI weight can be sub-dB. This value comes from 0.36 dB for the interfaces, 0.44 dB for the two MMIs, and 0.15 dB for a 0.5 mm BTO waveguide exhibiting 50% confinement factor. The inset of Figure 3(c) presents the envisaged cross-section of the rib-shaped BTO PS.

Conclusions

We present BTO-on-Si_3N_4 MZIs as weighting elements for neuromorphic photonics featuring ultra-low power consumption of 121 nW for π phase shift, an extinction ratio higher than 27dB, a $V_\pi L$ product as low as 2.94 Vmm and rise/fall times below 20 ns. The paper discusses also the role of the interface between the two platforms regarding the tradeoff between losses and power efficiency.

Acknowledgements

We wish to acknowledge EU funded NEBULA (Contract Number 871658) and ALLEGRO projects (Contract Number 101092766).

References

[1] G. Giamougiannis, A. Tsakyridis, M. Moralis-Pegios, G. Mourgias-Alexandris, A. R. Totovic, G. Dabos, M. Kirtas, N. Passalis, A. Tefas, D. Kalavrouziotis, D. Syrivellis, P. Bakopoulos, E. Mentovich, D. Lazovsky, and N. Pleros, "Neuromorphic silicon photonics with 50 GHz tiled matrix multiplication for deep-learning applications," *Advanced Photonics,* vol. 5, no. 1, pp. 016004, 2023, DOI: 10.1117/1.AP.5.1.016004 .

[2] J. Feldmann, N. Youngblood, M. Karpov, H. Gehring, X. Li, M. Stappers, M. Le Gallo, X. Fu, A. Lukaschuk, A. S. Raja, J. Liu, C. D. Wright, A. Sebastian, T. J. Kippenberg, W. H. P. Pernice, and H. Bhaskaran, "Parallel convolutional processing using an integrated photonic tensor core," *Nature*, vol. 589, no. 7840, pp. 52-58, 2021, DOI: 10.1038/s41586-020-03070-1.

[3] X. Xu, M. Tan, B. Corcoran, J. Wu, A. Boes, T. G. Nguyen, S. T. Chu, B. E. Little, D. G. Hicks, R. Morandotti, A. Mitchell, and D. J. Moss, "11 TOPS photonic convolutional accelerator for optical neural networks," *Nature*, vol. 589, no. 7840, pp. 44-51, 2021, DOI: 10.1038/s41586-020-03063-0.

[4] J. Joo, J. Park, and G. Kim,"Cost-Effective 2×2 Silicon Nitride Mach-Zehnder Interferometric (MZI) Thermo-Optic Switch," *IEEE Photonics Technology Letters*, vol. 30, no. 8, pp. 740-743, 2018, DOI: 10.1109/LPT.2018.2814616.

[5] S. T. Ilie, J. Faneca, I. Zeimpekis, T. Dominguez-Bucio, K. Grabska, D. W. Hewak, H. M. H. Chong, and F. Y. Gardes, "Thermo-optic tuning of silicon nitride microring resonators with low loss non-volatile Sb 2 S 3 phase change material," *Scientific Reports*, vol. 12, no. 1 pp. 17815, 2022, DOI: 10.1038/s41598-022-21590-w.

[6] A. S. Everhardt, T. L. A. Tran, C. Mitsolidou, T. R. Horner, R. Grootjans, R. Oldenbeuving, R. Heuvink, D. Geuzebroek, A. Leinse, C. Roeloffzen, and R. G. Heideman, "Ultra-low power stress-based phase actuation in TriPleX photonic circuits," *Integrated Optics: Devices, Materials, and Technologies XXVI*. Vol. 12004. SPIE, 2022, DOI: 10.1117/12.2609405 .

[7] H. Chen, Z. Zhao, Z. Zhang, G. Wang, J. Li, Z. Shang, M. Zhang, K. Guo, J. Yang, and P. Yan, "Heterogeneous integrated phase modulator based on two-dimensional layered materials," *Photonics Research*, vol. 10, no. 6, pp. 1401-1407, 2022, DOI: 10.1364/PRJ.453520.

[8] Y. Jiang, X. Han, H. Huang, P. Zhang, A. Dubey, H. Xiao, M. Yuan, A. Frigg, T. G. Nguyen, A. Boes, Y. Li, G. Ren, Y. Su, A. Mitchell, and Y. Tian, "Monolithic photonic integrated circuit based on silicon nitride and lithium niobate on insulator hybrid platform," *Advanced Photonics Research*, vol. 3, no. 10, pp. 2200121, 2022, DOI: 10.1002/adpr.202200121.

[9] J. E. Ortmann, F. Eltes, D. Caimi, N. Meier, A. A. Demkov, L. Czornomaz, J. Fompeyrine, and S. Abel, "Ultra-low-power tuning in hybrid barium titanate–silicon nitride electro-optic devices on silicon," *ACS Photonics,* vol. 6, no. 11, pp. 2677-2684, 2019, DOI: 10.1021/acsphotonics.9b00558.